

# Defective Rac-mediated proliferation and survival after targeted mutation of the $\beta_1$ integrin cytodomain

Emilio Hirsch,<sup>1,2</sup> Laura Barberis,<sup>1</sup> Mara Brancaccio,<sup>1</sup> Ornella Azzolino,<sup>1</sup> Dazhong Xu,<sup>5</sup> John M. Kyriakis,<sup>5</sup> Lorenzo Silengo,<sup>1,2</sup> Filippo G. Giancotti,<sup>6</sup> Guido Tarone,<sup>1,2</sup> Reinhard Fässler,<sup>3,4</sup> and Fiorella Altruda<sup>1,2</sup>

<sup>1</sup>Dipartimento di Genetica, Biologia, e Biochimica, Università di Torino, 10126 Torino, Italy

<sup>2</sup>Experimental Medicine Research Center, San Giovanni Battista Hospital, 10126 Torino, Italy

<sup>3</sup>Max-Planck Institute for Biochemistry, 8285 Martinsried, Germany

<sup>4</sup>Department of Experimental Pathology, Lund University Hospital, S-222 85 Lund, Sweden

<sup>5</sup>Diabetes Research Laboratory, Medical Services, Massachusetts General Hospital, Boston, MA 02129

<sup>6</sup>Cellular Biochemistry and Biophysics Program, Memorial Sloan-Kettering Cancer Center, New York, NY 10021

Cell matrix adhesion is required for cell proliferation and survival. Here we report that mutation by gene targeting of the cytoplasmic tail of  $\beta_1$  integrin leads to defective proliferation and survival both in vivo and in vitro. Primary murine embryonic fibroblasts (MEFs) derived from mutant homozygotes display defective cell cycle coupled to impaired activation of the FAK-PI3K-Akt and Rac-JNK signaling pathways. Expression in homozygous MEFs of a constitutively active form of Rac is able to rescue proliferation, survival, and JNK activation. Moreover, although

showing normal Erk phosphorylation, mutant cells fail to display Erk nuclear translocation upon fibronectin adhesion. However, expression of the constitutively activated form of Rac restores Erk nuclear localization, suggesting that adhesion-dependent Rac activation is necessary to integrate signals directed to promote MAPK activity. Altogether, our data provide the evidence for an epistatic interaction between the  $\beta_1$  integrin cytoplasmic domain and Rac, and indicate that this anchorage-dependent signaling pathway is crucial for cell growth control.

## Introduction

Modulation of cell adhesion is known to influence essential cellular processes such as proliferation, differentiation, and migration. Major molecular mediators of these effects are integrins, heterodimeric transmembrane glycoproteins able to link extracellular matrix components and intracellular actin cytoskeleton. Integrins are formed by  $\alpha$  and  $\beta$  subunits which act together (Hynes, 1992). So far, 8  $\beta$  and 18  $\alpha$  subunits have been described, and the  $\beta_1$  subunit is contained in 11 receptors with distinct  $\alpha$  chains. The  $\beta_1$  subunit is also present in alternatively spliced isoforms of the cytoplasmic C-terminal tail. Murine cells express a ubiquitous A and a muscle-specific D isoform (Belkin et al., 1996).

By binding to a large variety of interactors (Hemler, 1998; Liu et al., 2000), the short cytoplasmic sequence of all  $\beta_1$  variants regulates several kind of transmembrane signaling events (Sasry and Horwitz, 1993). The most membrane

proximal segment is encoded by a single exon (exon 6) that is shared by all  $\beta_1$  splice variants; it spans 25 amino acids able to interact with focal adhesion kinase (FAK),\* paxillin,  $\alpha$ -actinin, and melusin (Otey et al., 1993; Schaller et al., 1995; Brancaccio et al., 1999). On the other hand, each splice variant is characterized by the presence of distinct C-terminal ends. Amino acids of the  $\beta_{1A}$ -specific tail bind cytoskeletal components like talin and filamin (Pfaff et al., 1998) or signaling effectors like ICAP1 (Chang et al., 1997; Degani et al., 2002) and ILK (Dedhar and Hannigan, 1996) (Fig. 1).

The wide variety of cell adhesion events mediated by  $\beta_1$  integrins is crucial in vivo and essential for mammalian development (Fässler et al., 1996). Studies of anchorage-dependent cell growth suggest that integrins, together with growth factor receptors, activate mitogen-activated protein kinases and thus allow cell cycle progression. Adhesion to the extracellular matrix leads to the  $\alpha$  integrin subunit-

Address correspondence to Emilio Hirsch, Dipartimento di Genetica, Biologia, e Biochimica, Università di Torino, via Santena 5 bis, 10126 Torino, Italy. Tel.: 39-011-670-6680. Fax: 39-011-670-6547. E-mail: emilio.hirsch@unito.it

E. Hirsch and L. Barberis contributed equally to this work.

Key words: integrin; cytodomain; RAC; MAPK; proliferation

\*Abbreviations used in this paper: dpc, day(s) postcoitum; ES, embryonic stem; FAK, focal adhesion kinase; MEF, murine embryonic fibroblast; PFA, paraformaldehyde; SAPK, stress-activated protein kinase; TUNEL, TdT-mediated dUTP-biotin nick end labelin.

Common	Variable
~  KLLMI IHDRREFAKFEKEKMNAKWDT	GENPI YKSAVTTTVNPKYEGK
FAK Paxillin	Talin
$\alpha$ -Actinin Rack1 Melusin	ILK Filamin ICAP Myosin

Figure 1. **Known and inferred interactions of the  $\beta_1$  cytoplasmic domain.** Amino acids replaced in the  $\beta_{1de6}$  are boxed. See Hemler (1998) and Liu et al. (2000) for binding sites.

dependent activation of Fyn, and to the subsequent recruitment of Shc (Giancotti and Ruoslahti, 1999). In addition, the  $\beta$  integrin subunit is involved in the activation of the tyrosine kinase FAK. Both pathways are able to link adhesive events to the phosphorylation of Erk by activating Ras via direct binding of either FAK or Shc to Grb2 (Schlaepfer et al., 1994; Wary et al., 1996). Recently, it has been shown that FAK can also activate Erk through a mechanism involving B-Raf and Rap1 (Barberis et al., 2000). Although concerted Erk activation by adhesion and growth factors is con-

sidered necessary for Cyclin D1 induction (Roovers et al., 1999), some reports indicate that other adhesion-mediated signals are required for cell cycle progression (Le Gall et al., 1998). For example, in parallel to Erk activation, integrins trigger signals that allow the coupling of the Rac GTPase to its downstream effectors (del Pozo et al., 2000; Mettouchi et al., 2001).

Using a gene-targeting strategy in embryonic stem (ES) cells, we have isolated a  $\beta_1$  integrin allele encoding a mutant cytoplasmic domain ( $\beta_{1de6}$  allele) in which the alternatively spliced C-terminal sequence was substituted with 11 amino acids unrelated to all known  $\beta_1$  splice variants. Homozygous mice die between embryonic day 10.5 and 11.5. Moreover, mutant embryos show impaired cell proliferation and survival. Primary murine embryonic fibroblasts (MEFs) derived from mutant homozygotes display normal adhesion to fibronectin (Barberis et al., 2000) but exhibit strongly impaired integrin-mediated activation of PI3K, Rac, and JNK. In addition, mutant MEFs, although presenting normally phosphorylated Erk (Barberis et al., 2000), fail to translocate Erk into the nucleus. Erk nuclear localization, JNK activa-

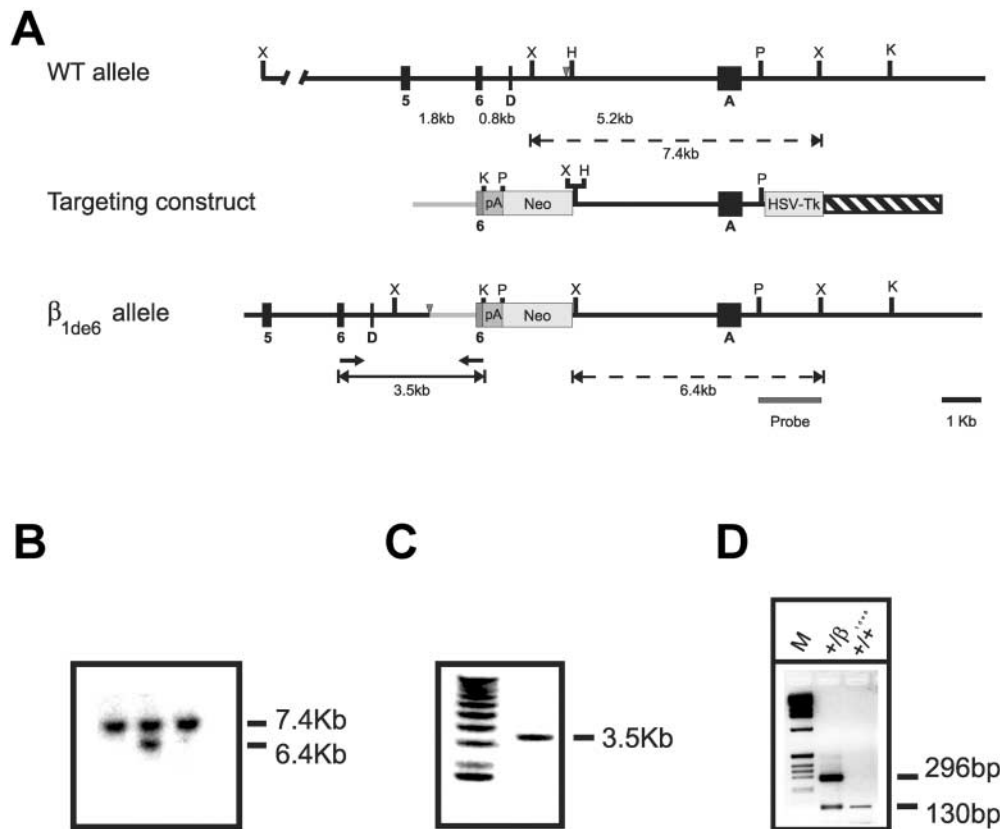
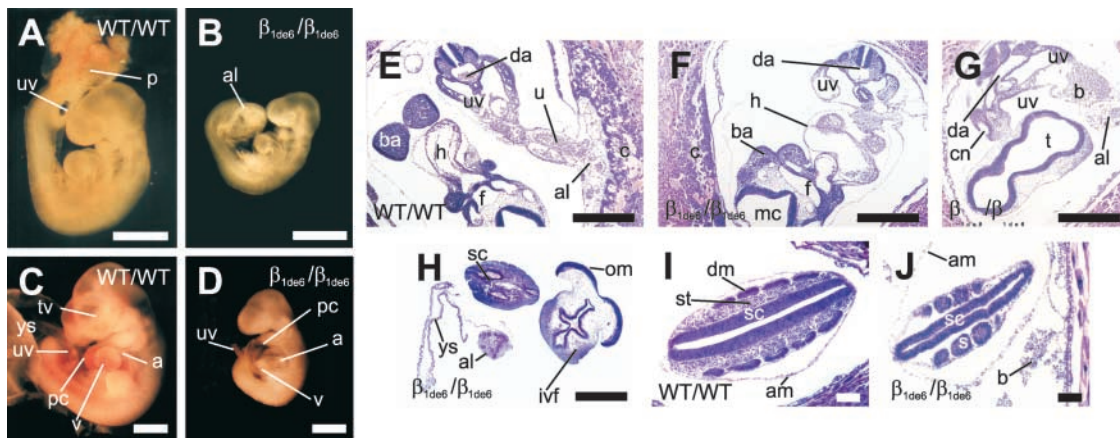


Figure 2. **Structure of the  $\beta_{1de6}$  locus.** (A) Schematic representation of the  $\beta_1$  integrin wild-type allele, of the targeting vector, and of the resulting  $\beta_{1de6}$  locus. Closed boxes represent  $\beta_1$  integrin exon 5, 6, and the alternatively spliced exon D and A. The size of introns is indicated. The solid arrows and bar below the  $\beta_{1de6}$  locus indicate the primers used for genomic amplification and the size of the resulting PCR product. The vertical arrowhead indicates the insertion site of the 5' of the construct. K, KpnI; H, HinDIII; P, Apal; X, XbaI. (B) Southern blot analysis of targeted ES cells. Genomic DNA was digested with XbaI. The targeted clone shows two bands corresponding to wild-type and mutant alleles, as expected after homologous recombination. (C) Exon 6 is duplicated in  $\beta_{1de6}$  cells. Genomic PCR with primers shown in panel a confirm the insertion of the mutant exon 6 downstream of its wild-type counterpart. (D) RT-PCR assay. In the heterozygous  $\beta_{1de6}$  RNA, primers on  $\beta_1$  integrin exon 5 and exon 6 amplify two fragments corresponding to the wild-type (exons 5 and 6; 130 bp) and the mutant (exons 5 and 6; mutant exon 6; 296 bp) mRNAs. Splicing of exon 6 to its duplicate causes a frameshift mutation and the substitution of the alternatively spliced C-terminal tail with 11 amino acids irrelevant to  $\beta_1$  integrin sequences. M:1kb ladder (GIBCO BRL).



**Figure 3. Phenotypic analysis of  $\beta_{1de6}$  homozygous embryos.** (A–D) Whole-mount wild-type (A and C) and mutant (B and D) embryos are shown at 9.5 (A and B) and 10.5 (C and D) dpc. (B) Mutant embryo displaying defective placentation. (D) Mutant embryos showing normal chorion–allantois fusion but cardiac defects. A reduction of the anterior–posterior axis and a significant disconnection between myocardium and pericardium is visible. (E–G) Histological analysis of 9.5-dpc embryos. (E) Wild-type embryo. (F and G) Mutant embryo showing lack of chorion–allantois fusion. Note that allantois and chorion are located on distinct planes and oppositely oriented. (H) Transverse section of the head of a  $\beta_{1de6}$  homozygous embryo at 10.5 dpc showing hindbrain exencephaly and lack of chorion–allantois fusion. (I) Section of the posterior trunk of a 10.5-dpc wild-type embryo. Somites already show differentiated dermomyotome and sclerotome. (J) Section of the back of a corresponding mutant embryo, showing retarded somite development and subsequent reduction of mesenchymal cells. Of note is the presence of hemorrhage in the exocoelom. a, atrium; al, allantois; am, amnion; b, primordial blood cells; ba, branchial arch; c, chorion; cn, caudal neuropore; da, dorsal aorta; dm, demomyotome component of somite; f, pharynx; h, heart; ivf, inter-ventricular foramen; mc, myelocoel; om, open myelencephalon; p, placenta; pc, pericardium; s, somites; sc, spinal cord; st, sclerotome component of somite; t, telencephalon; tv, telencephalic vesicle; u, umbilical stalk; uv, umbilical vessels; v, ventricle; ys, yolk sac. Bars: (A–H) 1 mm; (I) 200  $\mu$ m.

tion, and proliferation and survival are rescued by a constitutively active form of Rac, showing that  $\beta_1$  integrin–induced Rac activation is a crucial step for anchorage-dependent control of cell growth.

## Results

### Targeted mutation of the $\beta_1$ integrin cytoplasmic domain

A  $\beta_1$  integrin cytoplasmic domain mutant allele ( $\beta_{1de6}$ ) was obtained by gene targeting in murine ES cells. This allele was found in a single targeted clone, and consequently to a unique recombination event carried the duplication of exon 6 as indicated in Fig. 2. This structure lead to the expression of a  $\beta_1$  subunit in which the cytoplasmic sequence shared by all  $\beta_1$  integrin splice variants was followed by an irrelevant C-terminal tail sequence, consisting of 11 amino acids (with a predicted sequence: TVLLVPTSSQL) unrelated to all known  $\beta_1$  integrin isoforms.

### Homozygosity for the $\beta_{1de6}$ allele leads to embryonic lethality

ES cells deriving from the targeted clone carrying the  $\beta_{1de6}$  allele were injected into C57B6 host blastocysts, and germ line transmitting chimeras were generated. Heterozygous animals were viable and fertile. Histology of various tissues from these animals did not show any abnormality. Genotyping of litters derived from heterozygotes crosses showed that among 672 pups, 448 were heterozygous and 224 were wild-type homozygous. These results were consistent with a recessive embryonic lethal phenotype caused by homozygosity for the  $\beta_{1de6}$  allele.

Embryos derived from heterozygous intercrosses were dissected and genotyped by PCR. Homozygous mutants that were exteriorly indistinguishable from wild-type littermates could be identified until 8.5 d postcoitum (dpc). Later,  $\beta_{1de6}/\beta_{1de6}$  embryos started to exhibit retarded growth and a plethora of variably combined abnormalities. At 9.5 dpc, 50% of the mutant homozygous embryos showed the failure of the allantois to fuse with the chorion (Fig. 3, A and B). Histology of 9.5-dpc  $\beta_{1de6}$  homozygotes indicated that when the allantois was not fused to the chorion, embryos appeared abnormally oriented in the decidua (Fig. 3, C–E). At 10.5 dpc, 95% of mutants displayed cardiac and/or craniofacial abnormalities. Heart dysfunction was suggested by the presence of pericardiac effusion (Fig. 3, F and G). The severity of this phenotype was variable and ranged from mild liquid accumulation in the pericardial cavity to severe developmental retardation and pericardial swelling. In addition, mutants showed exencephaly (20% penetrance; Fig. 3 H) and/or abnormally waved or kinky neural tube (90% penetrance; Fig. 3 J). Moreover, mutant embryos exhibited blood leakage in the yolk sac, delayed somite development, and decreased density of mesenchymal cells (Fig. 3 J). At 11.5 dpc, mutant embryos showed no heart beating, appeared much smaller than wild-type littermates, and were already in process of being resorbed. At 12.5 dpc, no  $\beta_{1de6}$  homozygotes could be detected, and  $\sim 1/4$  of the implantation sites contained only blood. Identical results were obtained from the analysis of both C57/129Sv mixed genotype and 129Sv inbred intercrosses.

### The $\beta_{1de6}$ allele encodes a single $\beta_1$ integrin isoform which retains the ability to localize into focal contacts

To analyze whether  $\beta_{1de6}$  homozygous embryos were still able to express  $\beta_1$  integrin variants, RT-PCR analysis was

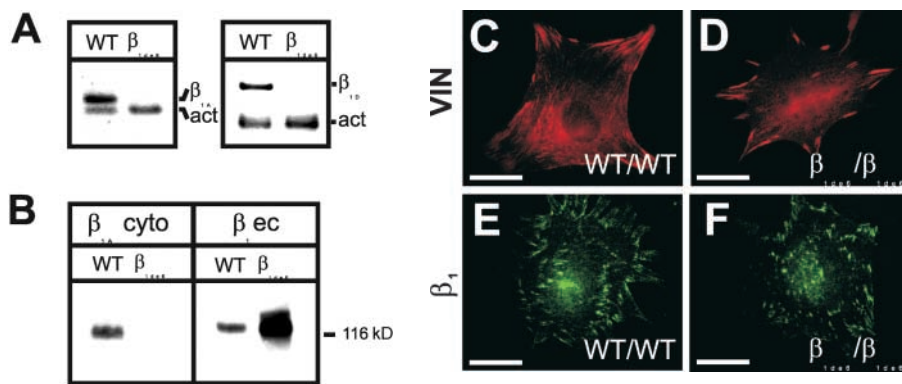


**Figure 4. Integrin expression in  $\beta_{1de6}$  homozygous MEFs.** (A) RT-PCR analysis of  $\beta_{1A}$  and  $\beta_{1D}$  splice variants in wild-type (WT) and  $\beta_{1de6}$  homozygous ( $\beta_{1de6}$ ) MEFs. A fragment of the actin (act) mRNA is coamplified as an internal control. (B) Immunoprecipitation of biotinylated cell surface  $\beta_1$  integrins. Extracts from wild-type (WT) and homozygous mutant ( $\beta_{1de6}$ ) MEFs were immunoprecipitated with an antibody recognizing the  $\beta_{1A}$ -specific cytoplasmic domain (left). The supernatant was subsequently immunoprecipitated with an antibody recognizing the  $\beta_1$

integrin extracellular portion (right panel). (C–F) Immunolabeling of wild-type (C and E) and mutant (D and F) MEFs. Vinculin (C and D) and  $\beta_1$  integrin subunit (E and F) staining are shown. Bars, 10  $\mu$ m.

performed to detect the presence of the  $\beta_{1A}$  and  $\beta_{1D}$  transcripts. Total RNA was extracted from mutant and wild-type embryos (9.5 dpc) and, as shown in Fig. 4 A,  $\beta_{1A}$  and  $\beta_{1D}$  could be amplified from wild-type RNA but not from  $\beta_{1de6}$  homozygous samples.

The expression of the mutant protein was analyzed by establishing cultures of MEFs isolated from 9.5 dpc embryos. To test the expression of the mutant integrin, the surface of wild-type and mutant MEFs was biotinylated, and extracts were immunoprecipitated using a polyclonal antiserum that recognized the  $\beta_{1A}$ -specific sequence. As indicated in Fig. 4 B (left),  $\beta_{1A}$  could be immunoprecipitated uniquely from wild-type cells. In contrast, a  $\beta_1$  integrin extracellular epitope could be detected in MEFs of both genotypes (Fig. 4 B, right). These data indicate that  $\beta_{1de6}$  homozygous cells expressed a single  $\beta_1$  integrin isoform carrying a mutant cytoplasmic domain. The alteration of the  $\beta_1$  C-terminal tail was previously associated with defective recruitment of the protein into focal contacts. Nevertheless, in agreement with a crucial role of  $\alpha$  subunits for integrin targeting to focal adhesions, immunofluorescence with anti-vinculin and anti- $\beta_1$  antibodies showed that, in mutant MEFs plated on fibronectin,  $\beta_{1de6}$  distributed in focal contacts as efficiently as wild-type  $\beta_1$  (Fig. 4, C–F).

Altogether, these data demonstrate that  $\beta_{1de6}$  is the only  $\beta_1$  integrin isoform expressed by homozygous mutant MEFs and that the altered cytoplasmic domain does not interfere with its correct cellular distribution.

### $\beta_{1de6}$ homozygotes and derived MEFs show impaired proliferation and survival

Integrin-mediated signaling is thought to control anchorage-dependent cell growth; thus, it is possible that  $\beta_{1de6}$  affects cell proliferation and survival. To test this hypothesis in vivo without being biased by a general defective growth due to abnormal materno-fetal circulation, 8.5-d-old embryos showing heart beating and normal placentation were studied. Counts of BrdU-labeled nuclei in wild-type and mutant embryos showed a small but significant 10% decrease of proliferating cells in  $\beta_{1de6}$  homozygotes (wild-type tissue:  $82 \pm 6$  BrdU-labeled nuclei/total nuclei per field  $\times 100$ ,  $n = 574$ ; mutant tissue:  $74 \pm 6$ ,  $n = 591$  – values expressed as mean  $\pm$  SD;  $P = 0.01$  by Student's  $t$  test). Strikingly, older embryos (9.5 dpc) showed a higher reduction of BrdU stain-

ing which was particularly evident in the mesenchyme (Fig. 5, A and B), where mutant cells exhibited a 30% decrease in the number of labeled nuclei (wild-type tissue:  $47 \pm 10$  BrdU labeled nuclei/total nuclei per field  $\times 100$ ,  $n = 8213$ ; mutant tissue:  $32 \pm 9$ ,  $n = 7433$  – values expressed as mean  $\pm$  SD;  $P = 0.03$  by Student's  $t$  test). In addition, detection by TdT-mediated dUTP-biotin nick end labeling (TUNEL) assay of apoptotic cells in sections of 9.5 dpc embryos revealed that mutant homozygotes also showed significantly higher numbers of TUNEL-positive cells in the mesenchyme and heart (Fig. 5, C and D).

Consistent with these findings,  $\beta_{1de6}$  homozygous MEFs showed a modified cell cycle profile. Whereas analysis of DNA content by FACS of synchronized mutant cells displayed a modest but statistically significant increase of cells in  $G_1$  (25% increment), the number of cells in S phase was lowered by 30% and cells in  $G_2$  were strongly reduced (76% decrease; Fig. 5 E). Moreover, testing of MEFs for adhesion-dependent cell proliferation indicated reduced numbers of BrdU labeled cells in cultures of mutant cells (Fig. 5 F). Interestingly, this proliferation defect was maximal on the  $\beta_1$  integrin ligand fibronectin but not on the  $\beta_3$  ligand vitronectin, thus showing the specificity of the defect (Fig. 5 F). Altogether, these data suggested that  $\beta_{1de6}$  homozygous MEFs were characterized by an impaired or delayed  $G_1/S$  transition. In agreement with this hypothesis, synchronized cultures showed that clearance of the cyclin dependent kinase inhibitor p27<sup>kip1</sup> together with accumulation of cyclin D1 occurred more slowly in mutant cells than in wild-type controls (Fig. 5 G).

In addition, in vitro analysis revealed in mutant MEFs reduced adhesion-mediated cell survival (Fig. 5 H). Consistent with these results, detection of caspase-3 activation in vivo (Fig. 5 I) exhibited, in  $\beta_{1de6}$  homozygous embryos, a significant decrease of inactive procaspase-3 and a concomitant increment of cleaved active caspase-3. These results demonstrate that the expression of  $\beta_{1de6}$  mutant integrin likely impairs anchorage-dependent signaling events that sustain cell proliferation and survival.

### The adhesion-triggered PI3K-dependent survival pathway is impaired in $\beta_{1de6}$ homozygous MEFs

Previous results revealed that  $\beta_{1de6}$  homozygous MEFs normally adhere to fibronectin but are not able to activate the tyrosine kinase FAK (Barberis et al., 2000). Be-

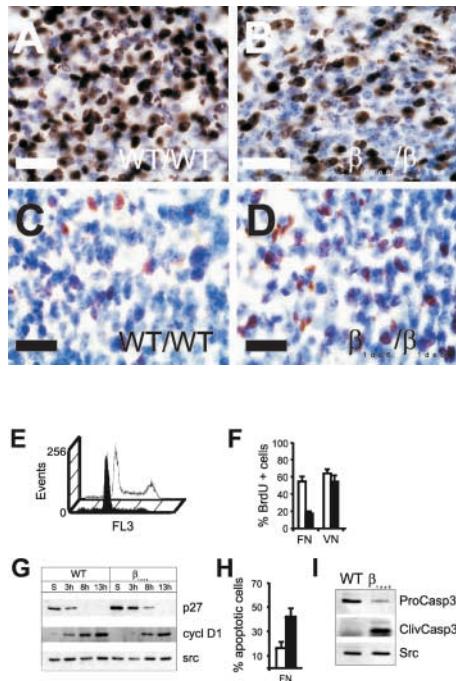


**Figure 5. Impaired proliferation and apoptosis in  $\beta_{1de6}$  homozygous embryos.** (A–D) Sections of wild-type (A and C) and mutant (B and D) 9.5 dpc embryos marked for BrdU (A and B) and TUNEL (C and D). Bars, 100  $\mu$ m. (E) Comparison of propidium iodide fluorescence peaks derived from nuclear DNA analysis of wild-type (white curve) and  $\beta_{1de6}$  homozygous (black curve) MEFs after 8 h of adhesion fibronectin in the presence of growth factors. Note the strong reduction of  $\beta_{1de6}$  homozygous MEFs in the G2/M cell cycle phase. (F) BrdU incorporation in wild-type (white bars) and mutant (black bars) MEFs. Proliferation was impaired in mutant MEFs after adhesion to the  $\beta_1$  integrin ligand fibronectin (FN) but not to the  $\beta_3$  ligand vitronectin (VN). (G) Analysis, in wild-type and  $\beta_{1de6}$  homozygous MEFs, of p27 and cyclin D1 after 3, 8, and 13 h of fibronectin adhesion in the presence of growth factors. Equal loading is indicated by Src immunoblotting. (H) Quantitation of wild-type (white bar) and mutant (black bar) apoptotic MEFs. (I) Analysis of the amount of the pro-caspase3 and its cleaved forms in total extracts from 10.5-dpc embryos. Data are representative of three (G and I) and four (E, F, and H) experiments.

cause FAK activity has been shown to regulate PI3K, a molecule involved in controlling proliferation and survival, we investigated whether the presence of  $\beta_{1de6}$  could interfere with adhesion-dependent PI3K activation. First, the ability of p85 PI3K regulatory subunit to coimmunoprecipitate with FAK was tested after adhesion to fibronectin. As shown in Fig. 6 A, recruitment of p85 to a FAK-containing complex was strongly reduced in  $\beta_{1de6}/\beta_{1de6}$  cells.

Next, PI3K activity induced by adhesion to fibronectin was tested by analyzing phosphorylation of the PI3K-dependent downstream target PKB/Akt. As shown in Fig. 6 C, whereas in wild-type cells PKB/Akt was activated by the adhesive stimulus, in  $\beta_{1de6}$  homozygous cells PKB/Akt phosphorylation was undetectable. Because activation of PI3K is crucial for PKB/Akt phosphorylation, these data strongly suggest that the  $\beta_1$  integrin cytoplasmic domain plays a crucial role in FAK-dependent PI3K activation.

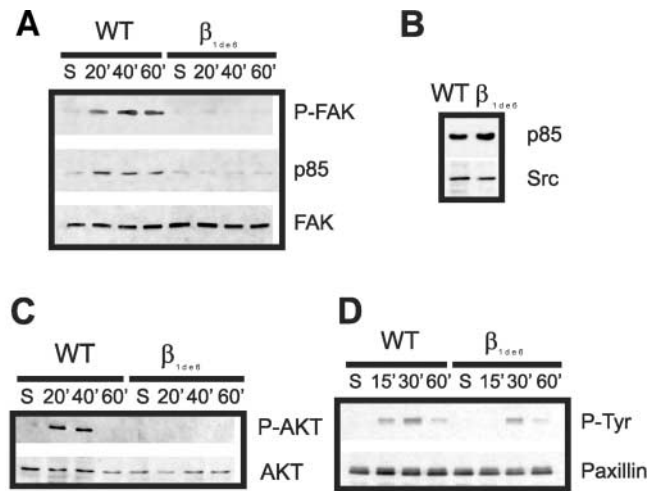


**Figure 6. Adhesion-dependent PI3K and paxillin activation.** (A) Extracts from wild-type (WT) and mutant ( $\beta_{1de6}$ ) MEFs, adhering to fibronectin for the given times, were immunoprecipitated with anti-FAK antibodies and were revealed by Western blot analysis of Tyr-phosphorylated FAK, p85 subunit of PI3K, and total FAK. (B) Detection of p85 in wild-type and mutant MEFs indicates identical expression levels. Equal loading was assayed by labeling with an anti-Src antibody. (C) Extracts from wild-type and mutant MEFs, adhering to fibronectin for the given times, were probed with anti PKB/Akt phosphorylated in Ser473, and total PKB/Akt. (D) After fibronectin adhesion, extracts derived from cells of the two genotypes were immunoprecipitated with an anti-paxillin antibody and revealed by Western blot analysis with the same anti-paxillin (paxillin) or with an anti-phosphotyrosine antibody (P-Tyr). (A–D) Data are representative of three experiments.

### $\beta_{1de6}$ affects Rac-dependent signaling

In fibroblasts, integrins contribute to the activation of the small GTPase Rac by triggering multiple signaling pathways, such as p130Cas/Crk/DOCK180 (Kiyokawa et al., 1998), PI3K/SOS (Mettouchi et al., 2001), and possibly paxillin activation (Igishi et al., 1999). Interestingly, analysis of adhesion-stimulated cells showed that paxillin phosphorylation is delayed and reduced in  $\beta_{1de6}$  homozygous MEFs (Fig. 6 D). Together with this observation, the lack of adhesion-stimulated activation of PI3K along with the previous observation that signaling through p130Cas is blocked (Barberis et al., 2000) suggested that, in mutant cells, Rac activation could be impaired. Indeed, pulldown assays using the CRIB domain of PAK-1 fused to GST revealed that, after plating  $\beta_{1de6}$  homozygous MEFs on fibronectin, Rac activation was heavily impaired both in the absence (Fig. 7 A) and in the presence (Fig. 7 B) of growth factors. Accordingly to this result, mutant cells analyzed by immunofluorescence at 30 min after fibronectin adhesion in the presence of growth factors showed decreased lamellipodia formation (Fig. 7 C).

Downstream, Rac stimulates the activation of JNK, a stress-activated protein kinase (SAPK) known to control cell proliferation and survival (Leppa and Bohmann, 1999). Activation of JNK and of another SAPK, p38, was thus examined in  $\beta_{1de6}$  homozygous MEFs. As shown in Fig. 7, D and E, plating on fibronectin stimulates the phosphorylation of

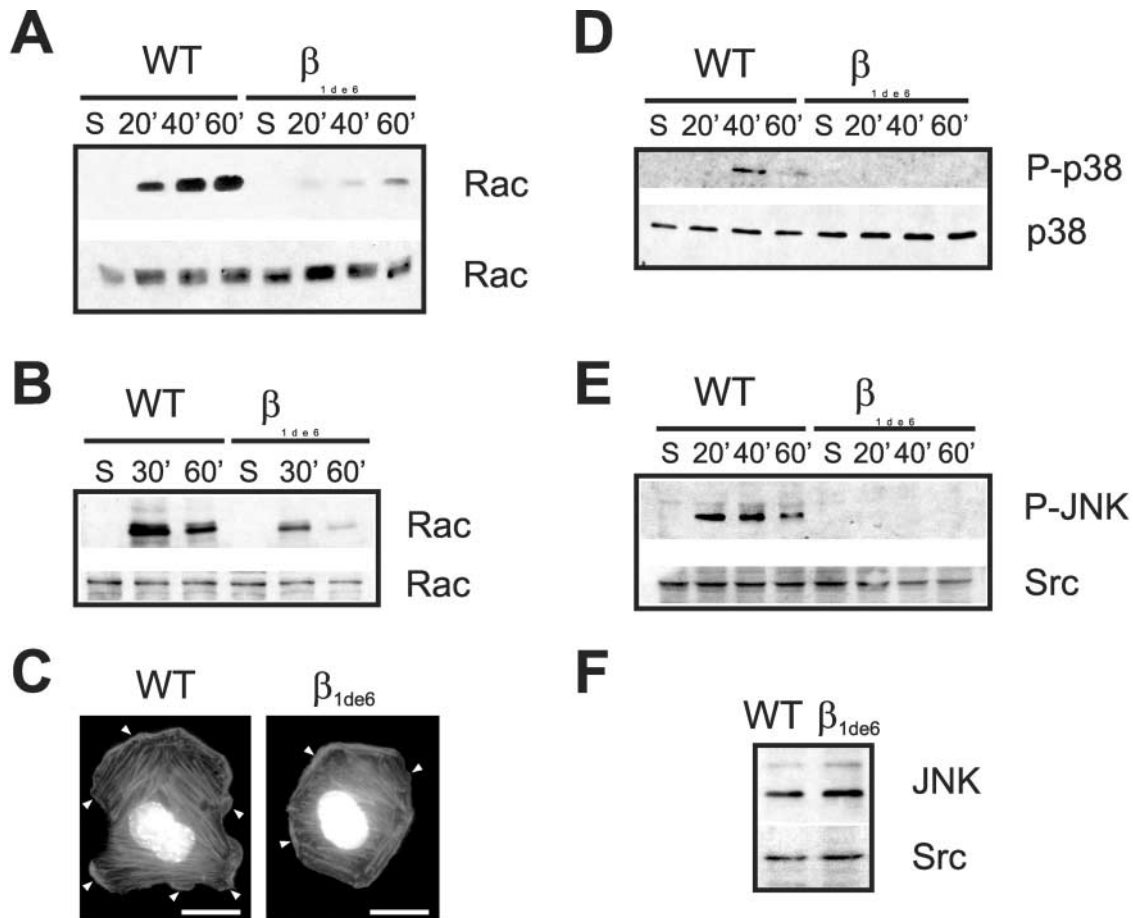


**Figure 7. Adhesion-mediated activation of Rac and SAPK.** Data are representative of four experiments. (A) Detection of Rac bound to the GST-PAK-1 CRIB domain after fibronectin adhesion for the given times. (B) The same as A but in the presence of 0.2% FCS and 6.25  $\mu\text{g/ml}$  insulin. (C) Analysis of lamellipodia (arrowheads) formation in wild-type (WT) and mutant ( $\beta_{1\text{de}6}$ ) MEFs. Starved cells were plated on fibronectin for 30' in the same conditions as in B. Actin cytoskeleton and nuclei were evidenced by phalloidin-RITC and bisbenzimidazole staining, respectively. Bars, 10  $\mu\text{m}$ . (D–E) Analysis of p38 (D) and JNK (E) SAPKs phosphorylation in wild-type and mutant MEFs treated as in A. (F) Western blot analysis of JNK in wild-type and mutant MEFs indicates identical expression levels. Equal loading was assessed by labeling with an anti-Src antibody.

both JNK and p38. In contrast, these activation events were undetectable in the mutant cells.

These data point to a crucial role for the C-terminal tail of  $\beta_1$  integrin in the activation of Rac and the subsequent phosphorylation of JNK.

#### Adhesion-activated Rac controls Erk subcellular localization and is essential for cell growth

To investigate whether impaired proliferation and survival in  $\beta_{1\text{de}6}$  homozygous embryos were caused by defective Rac activation, MEFs were infected with adenoviruses expressing a constitutively active (Rac<sup>V12</sup>) or a dominant negative (Rac<sup>N17</sup>) form of Rac.

After expression of Rac<sup>V12</sup>,  $\beta_{1\text{de}6}$  homozygous MEFs were able to activate JNK as efficiently as wild-type cells. Interestingly, Rac<sup>V12</sup> expression led to adhesion-independent JNK activation: similar JNK phosphorylation could be detected in both wild-type and mutant infected fibroblasts kept in suspension. Conversely, wild-type fibroblasts expressing Rac<sup>N17</sup> showed a strong reduction in activated JNK when adhering to fibronectin (Fig. 8 B).

Next, proliferation and survival were tested by BrdU and TUNEL assays in synchronized cell cultures of wild-type and mutant MEFs expressing Rac<sup>V12</sup>. As shown in Fig. 8, C and D, the proliferation defect and the increased apoptosis of mutant cells were completely rescued. On the other hand, the presence of Rac<sup>N17</sup> in wild-type MEFs was sufficient to cause the increased apoptosis and the reduced cell growth exhibited by untreated mutant MEFs.

In addition to JNK, Erk 1 and 2 play a crucial role in transducing mitogenic signals. MEFs homozygous for the  $\beta_{1\text{de}6}$  allele normally phosphorylate Erk in response to a combined stimulation by adhesion and growth factors (Barberis et al., 2000); however, in a large majority of these cells (85%;  $P \ll 0.001$  by  $\chi^2$  test versus wild-type controls;  $n = 300$  for each genotype) Erk nuclear translocation was strongly impaired (Fig. 9). Accordingly, forced Erk phosphorylation in suspended cells is not sufficient for nuclear translocation and activation of the transcription factor Elk (Aplin et al., 2001). To investigate the nature of the integrin-dependent signal required for Erk nuclear localization, we next examined whether Rac played a role in this process.

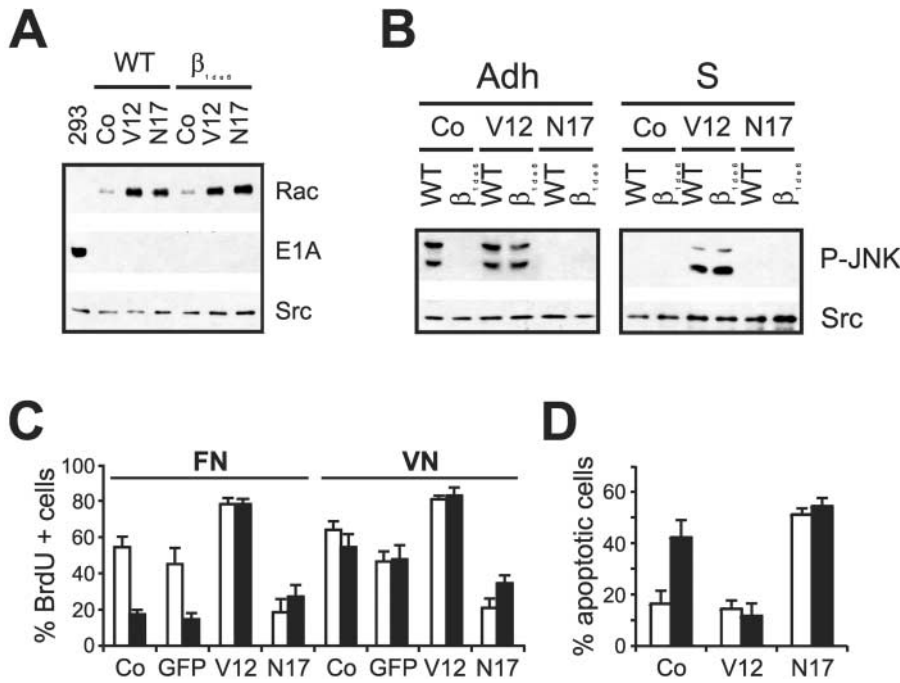


**Figure 8. Effects on cell proliferation and survival induced by expression of Rac<sup>V12</sup> and Rac<sup>N17</sup>.** (A) Expression of endogenous (Co) and exogenous Rac in MEFs infected with the constitutively active (V12) and the dominant negative (N17) forms of Rac. Infection with recombinant adenoviruses did not cause E1A viral protein expression. (B) Rac-dependent rescue of JNK phosphorylation in mutant MEFs after 30' of fibronectin adhesion (Adh) or suspension (S). (C) Evaluation of cell proliferation by BrdU incorporation in wild-type (white bars) and  $\beta_{1de6}$  homozygous (black bars) MEFs. Proliferation (Co) was impaired in mutant MEFs after adhesion to the  $\beta_1$  integrin ligand fibronectin (FN) but not to the  $\beta_3$  ligand vitronectin (VN). Infection with an adeno-GFP viral vector did not influence this effect (GFP). Expression of Rac<sup>V12</sup> rescued the defect. (D) In vitro analysis of apoptosis. Expression of Rac<sup>V12</sup> rescued mutant cells (black bars) from apoptosis, whereas the dominant negative form (N17) induced cell death in wild-type MEFs (white bars). Bar graphs represent means  $\pm$  SD of four independent experiments.

Strikingly, expression of Rac<sup>V12</sup> in  $\beta_{1de6}$  homozygous cells, adhering to fibronectin in the presence of growth factors, caused a strong enrichment of nuclear Erk; on the contrary, expression of Rac<sup>N17</sup> in wild-type cells decreased amounts of nuclear Erk (Fig. 9). Thus, integrin-dependent Rac activation is a critical step for Erk subcellular localization.

In conclusion, the findings presented here show an epistatic interaction between the  $\beta_1$  integrin cytoplasmic domain and Rac and demonstrate that this signaling pathway, by integrating JNK and Erk activation, plays an essential role in anchorage-dependent cell cycle progression, as well as cell survival.

## Discussion

Our study demonstrates that, in  $\beta_{1de6}$  homozygous mice, mutation of the C-terminal tail of the  $\beta_1$  integrin subunit causes in vivo and in vitro defective adhesion-dependent cell proliferation and survival and ultimately a recessive embryonic lethal phenotype.

Homozygous  $\beta_{1de6}$  embryos developed to midgestation but then died showing multiple variably penetrant phenotypes. Although these phenotypes could be analyzed in mice derived from a single ES clone, the chance that they were caused by a clonal artifact is very unlikely. In fact, they appeared stable and reproducible >30 generations in two distinct genetic backgrounds (inbred 129Sv and mixed 129Sv/C57B6), as well as after 10 generations of backcrossing with C57B6 mice. This stability, after such a dilution of the original ES clone genotype, supports the direct involvement of the  $\beta_{1de6}$  mutation in the reported phenotypes.

Interestingly,  $\beta_{1de6}$  homozygous embryos were found to survive longer than  $\beta_1$ -null mutants which die around embryonic day 5 (Fässler et al., 1996). Because the  $\beta_1$  integrin

cytoplasmic domain consists of a C-terminal tail that is subjected to alternative splicing and of a common juxtamembrane tract that is present in  $\beta_{1de6}$  and all  $\beta_1$  splice variants, our data suggest that the alternatively spliced region of the  $\beta_1$  cytoplasmic domain is dispensable in early morphogenetic processes. Likewise, our results indicate that the membrane proximal subdomain still present in the  $\beta_{1de6}$  integrin is sufficient to generate the signals and/or cytoskeletal linkage required for these events. Consistently, mice ectopically expressing  $\beta_{1D}$ , a muscle-specific splicing variant which also contains the wild-type common cytodomain, survive beyond implantation but die before birth because of variably penetrant phenotypes that, like in  $\beta_{1de6}$  homozygotes, include vascular and neuroepithelial malformations (Baudoin et al., 1998).

The presence in  $\beta_{1de6}$  homozygous embryos of vascular abnormalities and defective placentation suggests that this might be the reason for the lethality. Similar defects are the major causes of the death of mutant embryos lacking distinct integrin  $\alpha$  subunits like  $\alpha_4$  and  $\alpha_5$  (for review see Brakebusch et al., 1997). For example, the aberrant mesenchyme development (Fig. 3 J) and the leaking blood islands (Fig. 3, G and J) seen in  $\beta_{1de6}$  homozygotes have been similarly detected in  $\alpha_5$ -deficient embryos (Yang et al., 1993). However, the overall phenotype of  $\beta_{1de6}$  homozygotes, although sharing some characteristics of the  $\alpha_5$ -null embryos, strongly overlaps with that of  $\alpha_4$ -null mutants. In fact, like  $\beta_{1de6}/\beta_{1de6}$  embryos, mice lacking the  $\alpha_4$  integrin subunit die at embryonic day 11, showing variably penetrant phenotypes such as heart abnormalities and absence of chorion-allantois fusion (Yang et al., 1995). Although the explanation for this correspondence is not clear, on the basis that distinct  $\alpha$  integrin subunits show distinct biological properties, bind different intracellular proteins (Hemler, 1998; Liu

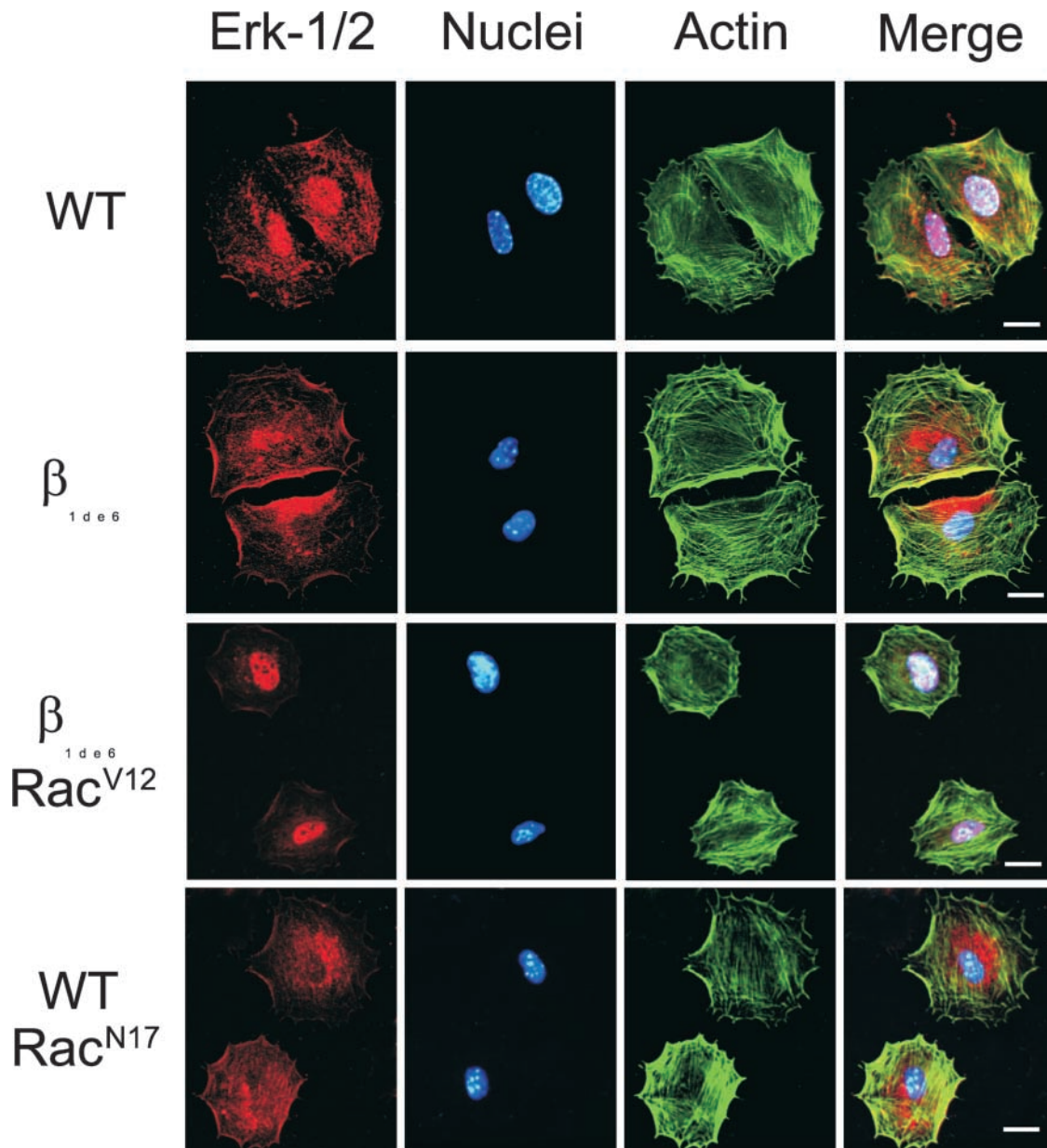


Figure 9. **Analysis by confocal microscopy of Erk nuclear accumulation.** Cells were seeded on fibronectin in the presence of growth factors for 4 h with or without prior infection with Rac<sup>V12</sup> or Rac<sup>N17</sup> adenoviruses. Fixed and permeabilized cells were stained with an anti-Erk1/2 polyclonal antibody (C-14; Santa Cruz Biotechnology), bisbenzamide, and phalloidin-FITC. Bar, 10  $\mu$ m.

et al., 2000) and specifically cooperate with the  $\beta_1$  cytodomain for signaling (Sastry et al., 1999), it is tempting to speculate that signaling of  $\alpha_4$  more strongly requires the  $\beta_1$  C-terminal tail than that of  $\alpha_5$ .

Despite the similarity between  $\beta_{1de6}/\beta_{1de6}$  and  $\alpha_4$ -null embryos, our analysis indicates that in vivo expression of  $\beta_{1de6}$  leads to defective cell proliferation and survival independently of the vascular phenotypes. In fact, decreasing numbers of dividing cells and increased apoptosis could be detected in  $\beta_{1de6}$  homozygous embryos that showed normal placentation and still had an apparently functional heart.

On the basis of in vitro experiments, it has been suggested that integrins may play a major role in allowing the G1-phase cell cycle progression (Assoian, 1997). The involve-

ment of integrins in permitting S phase entry has been highlighted by the requirement of adhesion and spreading onto extracellular matrix for triggering cyclin D1 accumulation and p27<sup>kip1</sup> decrease (Assoian and Schwartz, 2001). Furthermore, binding to distinct integrin ligands can selectively inhibit or promote cell growth (Giancotti, 2000). Nevertheless, extracellular matrix adhesion is a complex process in which several receptors other than integrins may contribute. The finding of signaling properties for transmembrane molecules like CD44 and syndecans (Couchman and Woods, 1999) complicates the assignment to integrins of cell matrix adhesion-triggered signals. Our results in vivo and in primary cell cultures clearly demonstrated that signaling from the  $\beta_1$  integrin cytodomain plays a central role in anchorage-

dependent cell growth. Consistent with a role of  $\beta 1$  integrin cytodomain in these processes, inhibitory effects on cell proliferation can be detected after transfection of immortalized cells with the  $\beta 1_C$  (Fornaro et al., 1995; Meredith et al., 1995) or the  $\beta 1_D$  (Belkin and Retta, 1998) splicing variants.

A requirement for integrin-mediated signal transduction is the clustering of these molecules into discrete subcellular domains like focal contacts. The finding that  $\beta 1_{de6}$  integrins localize into these districts was unexpected, as other  $\beta 1$  integrin C-terminal tail mutants have been reported to fail to enter focal adhesions. Nevertheless, similarly to  $\beta 1_{de6}$ , the  $\beta 1_B$  cytoplasmic domain variant can localize under specific conditions to a subset of focal contacts (Armulik et al., 2000). Because studies of  $\beta 1$  integrin cytodomain mutants have been carried out by transfection of transformed cell lines, the distribution of  $\beta 1_{de6}$  might be due to a specific behavior of primary MEFs. Alternatively, it is conceivable that specific adaptations allowing homozygous mutant cells to localize  $\beta 1_{de6}$  in focal contacts were selected during ontogeny. However, the recruitment of  $\beta 1_{de6}$  in focal adhesions excludes the possibility that the signaling defects observed in  $\beta 1_{de6}$  homozygous MEFs were caused by a displacement from the correct intracellular location. It is interesting to note that mutant MEFs used for localization experiments after adhering to fibronectin for 2 h appeared as spread as wild-type cells. This is in apparent contrast with the impaired Rac activation detected in  $\beta 1_{de6}$  homozygous fibroblasts. However, the immunofluorescence assays were performed in the presence of growth factors, a condition where Rac activation in mutant MEFs is decreased but not abolished. Therefore, it is possible that this residual Rac activity is sufficient to support cell spreading. Nonetheless, consistently with a deficient Rac activation, mutant cell showed a decreased spreading rate (Barberis et al., 2000) and displayed a reduced number of lamellipodia after 30 min of fibronectin adhesion.

Analysis of signaling properties of  $\beta 1_{de6}$  homozygous MEFs showed defective adhesion-triggered FAK, paxillin, PI3K, Rac, and JNK activation. Chen et al. (1996) have shown that FAK phosphorylation causes PI3K and PKB/Akt activation. This signaling pathway has been correlated to the protection from apoptosis induced by detachment from the extracellular matrix (anoikis) (Frisch and Ruoslahti, 1997). Because activated PKB/Akt is known to regulate apoptosis by phosphorylating pro-apoptotic molecules such as BAD and caspase 9 (Datta et al., 1999), the increased apoptosis in  $\beta 1_{de6}/\beta 1_{de6}$  MEFs might depend on the defective activation of PI3K/PKB/Akt.

Recently, PI3K has been found to play an essential role in adhesion-dependent Rac activation in endothelial cells (Mettouchi et al., 2001). This process is mediated by the guanine nucleotide exchange factor SOS that, in the presence of PI3K products, becomes an activator of Rac. However, it has been reported that in fibroblasts, a second pathway, requiring interaction of p130Cas, Crk, and DOCK180 plays a prominent role in Rac activation. Because p130Cas is not activated in  $\beta 1_{de6}$  homozygous MEFs (Barberis et al., 2000), we could not define the respective contribution of these two pathways. Nevertheless, the signaling pathway triggered by p130Cas has central role in promoting matrix-

dependent survival. Adhesion-dependent p130Cas phosphorylation and recruitment of Crk trigger antiapoptotic signals which are relayed by the subsequent activation of Rac and Jnk (Dolfi et al., 1998). In addition, Almeida et al. (2000) reported that the Cas-Rac-PAK-MKK4-JNK route is activated by fibronectin adhesion and promotes survival of primary fibroblasts. In agreement, the finding that Rac rescues  $\beta 1_{de6}$  homozygous MEFs from programmed cell death, further supports the notion that the FAK-Cas-Rac-JNK pathway plays a fundamental role in preventing anoikis.

Interestingly, although FAK is not activated in  $\beta 1_{de6}/\beta 1_{de6}$  MEFs, the lack of FAK in mice results in an embryonic lethal phenotype that is much more severe than that of  $\beta 1_{de6}$  homozygotes. FAK-null embryos do not develop beyond 8 dpc and show strong deficits in mesenchymal development apparently linked to impaired migration of mesodermal cells (Furuta et al., 1995). The differences in phenotype between FAK-null and  $\beta 1_{de6}$  homozygotes suggest that the abnormal adhesion-dependent signaling in  $\beta 1_{de6}/\beta 1_{de6}$  MEFs likely does not only depend on the deficit in FAK phosphorylation. Consistently,  $\beta 1_{de6}$  homozygous MEFs showed a defective activation of other important signaling pathways, possibly leading to Rac activation such as those arising from paxillin. The future study of the effects caused by expression of a dominant positive FAK in  $\beta 1_{de6}$  homozygous MEFs will be instrumental to address the specific role of FAK in this system.

Conversely, the rescue of the proliferation defect shown by  $\beta 1_{de6}$  mutant cells by an activated Rac demonstrated a central role of this GTPase in anchorage-dependent signaling. Consistent with this finding, Rac activation has been found to be essential, in endothelial cells, to promote adhesion-dependent Cyclin D1 accumulation and progression through the G<sub>1</sub> phase (Mettouchi et al., 2001). The precise mechanism by which Rac controls cell cycle progression is still unclear. Nevertheless, our data indicated that adhesion-induced Rac activation is necessary for the phosphorylation of the Rac downstream effector JNK. The role of JNK in controlling cell proliferation and survival is controversial. However, several experimental evidences suggest its implication in the activation of genes involved in cell cycle progression. For example, fibroblasts lacking the JNK substrate c-Jun show a severe proliferation defect (Johnson et al., 1993). Furthermore, adhesion-dependent JNK activation is necessary for progression through the G<sub>1</sub> phase of the cell cycle (Oktay et al., 1999).

It has been previously shown that  $\beta 1_{de6}$  homozygous MEFs normally activate Erk in response to a combined stimulation by adhesion and growth factors (Barberis et al., 2000). However, the results reported here showed that this event is not sufficient to promote cell cycle progression, and that other integrin-dependent signals deriving from Rac are crucially required. The role of adhesion-triggered Erk activation in cell proliferation is indeed controversial: whereas Roovers et al. (1999) propose that artificial activation of Erk in suspended cells can override adhesive requirements for cell cycle progression, Le Gall et al. (1998) show that these conditions are not sufficient to induce Cyclin D1 expression. In addition, recent experiments show that, independently from adhesion, Erk phosphorylation per se is not suf-

ficient for nuclear translocation and activation of the transcription factor Elk (Aplin et al., 2001). Analysis of Erk subcellular localization revealed that, after adhesion to fibronectin, homozygous  $\beta_{1de6}$  MEFs fail to translocate phosphorylated Erk into the nuclei. Interestingly, this defect could be rescued by the expression of a constitutively activated Rac. Such findings conclusively indicate that Erk nuclear translocation requires adhesion-mediated Rac activation. Further studies will be required to define the precise biochemical mechanism underlying this process.

At present, the possibility that the substitution of the  $\beta_1$  C-terminal tail by 11 amino acids provided a specific ability to positively induce the described signaling defects cannot be formally excluded. However, the chances that the 11 random amino acids result in an intrinsic signaling activity leading to FAK-Rac-JNK/Erk inhibition are objectively poor. In fact, scanning of existing protein domain and human genome databases failed to indicate any significant homology of the  $\beta_{1de6}$ -specific sequence to other naturally occurring proteins. Moreover, the signaling properties of  $\beta_{1de6}$  are consistent with what described for several different  $\beta_1$  integrin cytoplasmic domain mutants (Sasstry and Horwitz, 1993). In particular, the mutant that specifically lacks the alternatively spliced C-terminal tail, like  $\beta_{1de6}$ , does not activate FAK (Retta et al., 1998). Finally, the phenotypic rescue by expression of a constitutively active form of Rac further strengthens the hypothesis that the  $\beta_{1de6}$  mutation causes a loss of function effect, specifically affecting integrin-mediated signals. In conclusion, the findings presented here provide a genetic link between the  $\beta_1$  integrin cytoplasmic domain and the adhesion-mediated activation of Rac, thus supporting the notion that if integrins fail to trigger signals leading to MAPK activity, cell cycle progression as well as cell survival are impaired *in vivo*.

## Materials and methods

### Generation of $\beta_{1de6}$ mutant ES cells and mice

To generate the targeting construct aimed at producing a truncated  $\beta_1$  cytoplasmic domain, a 5' homology arm was obtained by PCR amplification of the intron between murine  $\beta_1$  integrin exon 5 and 6 (1.8 kbp), using two primers hybridizing to the intron downstream exon 5 (5'-GGAATTCCTC-GAGCTGAGTCATTGCTGGGGTTC-3') and to the end of exon 6 (5'-GGAATTCATCAGGTGTCCCACTTGGCATTTC-3'), respectively. Stop codons, a PGK polyadenylation sequence, and a neomycin resistance cassette were inserted downstream. The 3' homology arm consisted in a 4-kbp Hind III-Apa I fragment of the murine  $\beta_1$  gene derived from a 129Sv mouse strain genomic clone. After transfection and selection of G418-resistant R1 ES cells, homologous recombinants were screened by Southern blot, probing XbaI-digested DNA with an Apa I-XbaI genomic fragment external to the construct. A single clone showing the restriction pattern expected by the homologous recombination event was microinjected in C57B6 blastocysts and germ line-transmitting chimeras were used to generate inbred 129Sv and outbred 129Sv/C57B6 mutant strains.

### Characterization of the $\beta_{1de6}$ locus and integrin expression analysis

Southern blot analysis of  $\beta_{1de6}$  heterozygous DNA with a neomycin probe confirmed single copy insertion of the construct but also indicated that the left arm of the targeting construct had integrated downstream the endogenous exon D (Fig. 2 A). This integration event was confirmed by PCR using two oligonucleotides corresponding to exon 6 in forward and reverse direction (P1: 5'-ATTGGGATGATGTCGGGACC-3'; P2: 5'-AGGCGTGGT-TGCTGGAATTG-3') and the Expand Long Template PCR system (Boehringer Mannheim) (Fig. 2 C). The amplified fragment was cloned and sequenced with an ABI-Prism (Perkin Elmer) sequencing machine. The

break-point site was identified by comparing this sequence with the sequence of the wild-type intron between exon 5 and 6. These sequences were used for the design of three oligonucleotides (P3: 5'-CTTATGTC-CCTATCCTCTGC-3'; P4: 5'-TCTCCCTAGGTGTTGTACC-3'; P5: 5'-GGCACTTGCTAACAAGACTG-3') which allowed mouse genotyping by genomic PCR. The P3-P4 and P3-P5 couples amplified the  $\beta_1$  wild-type allele and the  $\beta_{1de6}$  allele, respectively. RT-PCR experiments (Fig. 2 D) were performed on total RNA of heterozygous ES cells using oligonucleotides located in exon 5 and 6 (5'-AGGACATTGATGACTGCTGG-3' and P1, respectively).

For the detection of  $\beta_{1A}$  and  $\beta_{1D}$  expression, total RNA was extracted from 10.5-d-old embryos using the RNeasy mini kit (QUIAGEN) and retrotranscribed using random primers (Amersham Pharmacia Biotech). Yolk sacs were used to genotype the embryo. Oligonucleotide couples were designed to amplify either  $\beta_{1A}$  (P1: 5'-AGGACATTGATGACTGCTGG-3'; P2: 5'-CGGGATC-CAAATCCGCTGAGTAGG-3'),  $\beta_{1D}$  (P1; P3: 5'-AAACTCAGAGAC-CAGCTTAC-3') or actin (5'-TCGACATCAGGAAGGACCTGT-3'; 5'-GAGGTGGAGTGTGTCTAGAAG-3'), in a multiplexed reaction consisting of 10 cycles of touch down protocol (annealing from 65°C to 55°C) followed by 17 cycles (95°C 30 s, 55°C 30 s, and 72°C 30 s) for  $\beta_{1A}$  and 19 cycles for  $\beta_{1D}$ .

To detect wild-type and mutant  $\beta_1$  proteins, embryonic fibroblasts were harvested and washed in Hank's buffer (1.3 mM CaCl<sub>2</sub>, 0.4 mM MgSO<sub>4</sub>, 5 mM KCl, 138 mM NaCl, 5.6 mM D-glucose, 25 mM Hepes, pH 7.4). Cells were biotinylated at their surface for 30 min at 4°C, washed three times, lysed in TBS-Triton 0.5%, and centrifuged 10 min. 500  $\mu$ g of extract were first precipitated with anti- $\beta_{1A}$  and subsequently with an anti- $\beta_1$  integrin recognizing the extracellular domain.

### Morphological and histological analysis

Embryos were dissected and fixed in 2% formalin in PBS. Whole-mount specimens were examined and photographed under the stereomicroscope (Wild). For histological analysis, the whole decidua or dissected embryos were fixed in Carnoy's solution for 4–6 h at 4°C. Paraffin sections (5  $\mu$ m) were analyzed after haematoxylin-eosin staining.

### Analysis of phenotypes in embryonic fibroblasts

For MEF cultures, 9.5-d-old embryos were dissected from maternal tissue in sterile PBS and individually incubated in trypsin (0.5 ml/embryo). Dissociated tissue was plated in the presence of DME 10% FCS. After 1 wk in culture, cells were expanded to generate a homogeneous cell population. For the subsequent experiments mutant and wild-type cells derived for 2–3 embryos were pooled and passaged maximally five times. Assays were confirmed with at least three different cell populations.

To monitor integrin signaling, cells were deprived of growth factors for 24 h, detached, and washed. The cells were either lysed immediately or plated on fibronectin 15  $\mu$ g/ml for the indicated times and lysed. Extraction buffer consisted of 25 mM tris-HCl, pH 7.5, 1% Triton X-100, 150 mM NaCl, 1 mM Na<sub>3</sub>VO<sub>4</sub>, 10 mM NaF, 1 mM Na<sub>4</sub>P<sub>2</sub>O<sub>7</sub> and 1 mM EDTA. The Rac pulldown assay was performed as described (Mettouchi et al., 2001).

### Immunofluorescence assays and Erk subcellular localization analysis

MEFs were detached with EDTA 3 mM, washed twice, and replated on fibronectin-coated dishes. After a 4-h adhesion, cells were fixed in 2% paraformaldehyde (PFA), permeabilized with TBS 0.3%-Triton, blocked with TBS 5%-BSA, and stained for 1 h with the primary antibody and 45 min with a rhodamine or fluorescein conjugated secondary antibody. For analysis of lamellipodia formation, cells were starved for 24 h, detached and replated as above in the presence of 0.2 FCS and 6.25  $\mu$ g/ml insulin. After 30 min, cells were fixed in 2% PFA, stained with phalloidin-RITC and bisbenzimidazole, and photographed. For Erk subcellular localization, MEFs were starved 24 h in the absence or in presence of adenoviral infection (carrying V12 or N17 forms of Rac). Cells were detached with EDTA 3 mM, washed twice and replated on fibronectin coated dishes for 4 h in the presence of growth factors. Cells were fixed with PFA 2%, permeated with TBS 0.3%-Triton, blocked with TBS 5%-BSA, stained ON at 4°C with a polyclonal antibody recognizing Erk (Cat: SC-16; Santa Cruz Biotechnology), washed again in TBS, and stained for 1 h with a rhodamine-conjugated anti-rabbit antibody mixed to a fluorescein-conjugated phalloidin. After TBS washing, cells were incubated 5 min with bisbenzimidazole (1  $\mu$ g/ml). Fluorescence was detected using a confocal microscope.

### Proliferation and apoptosis assays

For *in vivo* BrdU labeling, embryos were dissected from maternal tissues at 8.5 and at 9.5 dpc 1 h after intraperitoneal injection of 10  $\mu$ g/g body weight of 5-bromo-2'-deoxy-uridine (BrdU; Sigma-Aldrich). For cell prolif-

eration assays, cells were starved 24 h in absence of serum, detached, and replated for 8 h on 15  $\mu\text{g}/\text{ml}$  matrix-coated dishes in the presence of 0.2% FCS, 6.25  $\mu\text{g}/\text{ml}$  insulin, and 10  $\mu\text{M}$  BrdU. MEFs were fixed with 4% PFA and stained using the BrdU detection kit II (Roche). For FACS analysis of DNA content, cells treated as above were stained with propidium iodide using the Cycle TEST PLUS DNA Reagent Kit (Becton Dickinson). To detect apoptosis, cells or sections of 9.5-dpc embryos were treated in the same way and analyzed by a TUNEL assay using the In Situ Cell Death Detection POD Kit (Roche).

### Recombinant adenoviruses and rescue experiments

Recombinant adenoviruses expressing GFP or cDNAs for RAC in constitutively active (V12) and dominant negative (N17) forms were constructed. Infection of 293 cells was monitored by GFP expression, and when ~90% of the cells were floating, the pellet was freeze thawed three times to liberate the virus. MEFs were infected by 100  $\mu\text{l}$  of virus stock generating at least the infection of 60% of the cells. E1A expression was monitored to exclude the presence of revertant adenoviruses. GFP-positive infected cells were analyzed for proliferation and survival as above.

### Antibodies

Anti P-Tyr PY20, anti-Src, anti-cleaved Caspase-3, anti-Prodomain of Caspase-3, anti-E1A, anti-p27 and anti-Cyclin D1 were purchased from Santa Cruz Biotechnology; anti-paxillin, anti-p85, and anti-RAC were purchased from Transduction Laboratories; and anti-JNK, anti-P-JNK, anti-AKT, anti-P-AKT, anti-p38, and anti-P-p38 were purchased from New England Biolabs.

We wish to thank Sarah Forno and Immacolata Carfora for technical assistance. We are grateful to Bosco Chan (The John P. Roberts Research Institute, London, Canada), Dietmar Vestweber (ZMBE University, Muenster, Germany), and Arnoud Sonnenberg (Netherlands Cancer Institute, Amsterdam, Netherlands) for providing anti-integrin antibodies. We thank Fiorella Balzac, Paola Defilippi and Alexander Pfeifer for helpful discussion.

This work was supported by grants from the National Research Council (Target Project on Biotechnology) and from the Ministry of University and Scientific research to F. Altruda, from AIRC to G. Tarone, and from the Swedish National Science Foundation to R. Fässler.

Submitted: 19 November 2001

Revised: 20 March 2002

Accepted: 20 March 2002

## References

- Almeida, E.A., D. Ilic, Q. Han, C.R. Hauck, F. Jin, H. Kawakatsu, D.D. Schlaepfer, and C.H. Damsky. 2000. Matrix survival signaling: from fibronectin via focal adhesion kinase to c-Jun NH(2)-terminal kinase. *J. Cell Biol.* 149:741–754.
- Aplin, A.E., S.A. Stewart, R.K. Assoian, and R.L. Juliano. 2001. Integrin-mediated adhesion regulates ERK nuclear translocation and phosphorylation of Elk-1. *J. Cell Biol.* 153:273–282.
- Armulik, A., G. Svineng, K. Wennerberg, R. Fassler, and S. Johansson. 2000. Expression of integrin subunit beta1B in integrin beta1-deficient GD25 cells does not interfere with alphaVbeta3 functions. *Exp. Cell Res.* 254:55–63.
- Assoian, R.K. 1997. Anchorage-dependent cell cycle progression. *J. Cell Biol.* 136:1–4.
- Assoian, R.K., and M.A. Schwartz. 2001. Coordinate signaling by integrins and receptor tyrosine kinases in the regulation of G1 phase cell-cycle progression. *Curr. Opin. Genet. Dev.* 11:48–53.
- Barberis, L., K.K. Wary, G. Fiucci, F. Liu, E. Hirsch, M. Brancaccio, F. Altruda, G. Tarone, and F.G. Giancotti. 2000. Distinct roles of the adaptor protein Shc and focal adhesion kinase in integrin signaling to ERK. *J. Biol. Chem.* 275:36532–36540.
- Baudoin, C., M.J. Goumans, C. Mummery, and A. Sonnenberg. 1998. Knockout and knockin of the beta1 exon D define distinct roles for integrin splice variants in heart function and embryonic development. *Genes Dev.* 12:1202–1216.
- Belkin, A.M., and S.F. Retta. 1998. beta1D integrin inhibits cell cycle progression in normal myoblasts and fibroblasts. *J. Biol. Chem.* 273:15234–15240.
- Belkin, A.M., N.I. Zhidkova, F. Balzac, F. Altruda, D. Tomatis, A. Maier, G. Tarone, V.E. Koteliansky, and K. Burridge. 1996. Beta 1D integrin displaces the  $\beta 1A$  isoform in striated muscles: localization at junctional structures and signaling potential in nonmuscle cells. *J. Cell Biol.* 132:211–226.
- Brakebusch, C., E. Hirsch, A. Potocnik, and R. Fassler. 1997. Genetic analysis of beta1 integrin function: confirmed, new and revised roles for a crucial family of cell adhesion molecules. *J. Cell Sci.* 110:2895–2904.
- Brancaccio, M., S. Guazzone, N. Menini, E. Sibona, E. Hirsch, M. De Andrea, M. Rocchi, F. Altruda, G. Tarone, and L. Silengo. 1999. Melusin is a new muscle-specific interactor for beta(1) integrin cytoplasmic domain. *J. Biol. Chem.* 274:29282–29288.
- Chang, D.D., C. Wong, H. Smith, and J. Liu. 1997. ICAP-1, a novel  $\beta 1$  integrin cytoplasmic domain-associated protein, binds to a conserved and functionally important NPXY sequence motif of beta1 integrin. *J. Cell Biol.* 138:1149–1157.
- Chen, H.C., P.A. Appeddu, H. Isoda, and J.L. Guan. 1996. Phosphorylation of tyrosine 397 in focal adhesion kinase is required for binding phosphatidylinositol 3-kinase. *J. Biol. Chem.* 271:26329–26334.
- Couchman, J.R., and A. Woods. 1999. Syndecan-4 and integrins: combinatorial signaling in cell adhesion. *J. Cell Sci.* 112:3415–3420.
- Datta, S.R., A. Brunet, and M.E. Greenberg. 1999. Cellular survival: a play in three Acts. *Genes Dev.* 13:2905–2927.
- Dedhar, S., and G.E. Hannigan. 1996. Integrin cytoplasmic interactions and bidirectional transmembrane signalling. *Curr. Opin. Cell Biol.* 8:657–669.
- Degani, S., F. Balzac, M. Brancaccio, S. Guazzone, S.F. Retta, L. Silengo, A. Eva, and G. Tarone. 2002. The integrin cytoplasmic domain-associated protein ICAP-1 binds and regulates Rho family GTPases during cell spreading. *J. Cell Biol.* 156:377–388.
- del Pozo, M.A., L.S. Price, N.B. Alderson, X.D. Ren, and M.A. Schwartz. 2000. Adhesion to the extracellular matrix regulates the coupling of the small GTPase Rac to its effector PAK. *EMBO J.* 19:2008–2014.
- Dolfi, F., M. Garcia-Guzman, M. Ojaniemi, H. Nakamura, M. Matsuda, and K. Vuori. 1998. The adaptor protein Crk connects multiple cellular stimuli to the JNK signaling pathway. *Proc. Natl. Acad. Sci. USA.* 95:15394–15399.
- Fässler, R., E. Georges-Labouesse, and E. Hirsch. 1996. Genetic analyses of integrin function in mice. *Curr. Opin. Cell Biol.* 8:641–646.
- Fornaro, M., D.Q. Zheng, and L.R. Languino. 1995. The novel structural motif Gln795-Gln802 in the integrin beta 1C cytoplasmic domain regulates cell proliferation. *J. Biol. Chem.* 270:24666–24669.
- Frisch, S.M., and E. Ruoslahti. 1997. Integrins and anoikis. *Curr. Opin. Cell Biol.* 9:701–706.
- Furuta, Y., D. Ilic, S. Kanazawa, N. Takeda, T. Yamamoto, and S. Aizawa. 1995. Mesodermal defect in late phase of gastrulation by a targeted mutation of focal adhesion kinase, FAK. *Oncogene.* 11:1989–1995.
- Giancotti, F.G. 2000. Complexity and specificity of integrin signalling. *Nat. Cell Biol.* 2:E13–E14.
- Giancotti, F.G., and E. Ruoslahti. 1999. Integrin signaling. *Science.* 285:1028–1032.
- Hemler, M.E. 1998. Integrin associated proteins. *Curr. Opin. Cell Biol.* 10:578–585.
- Hynes, R.O. 1992. Integrins: versatility, modulation, and signaling in cell adhesion. *Cell.* 69:11–25.
- Igishi, T., S. Fukuhara, V. Patel, B.Z. Katz, K.M. Yamada, and J.S. Gutkind. 1999. Divergent signaling pathways link focal adhesion kinase to mitogen-activated protein kinase cascades. Evidence for a role of paxillin in c-Jun NH(2)-terminal kinase activation. *J. Biol. Chem.* 274:30738–30746.
- Johnson, R.S., B. van Lingen, V.E. Papaioannou, and B.M. Spiegelman. 1993. A null mutation at the c-jun locus causes embryonic lethality and retarded cell growth in culture. *Genes Dev.* 7:1309–1317.
- Kiyokawa, E., Y. Hashimoto, S. Kobayashi, H. Sugimura, T. Kurata, and M. Matsuda. 1998. Activation of Rac1 by a Crk SH3-binding protein, DOCK180. *Genes Dev.* 12:3331–3336.
- Le Gall, M., D. Grall, J.C. Chambard, J. Pouyssegur, and E. Van Obberghen-Schilling. 1998. An anchorage-dependent signal distinct from p42/44 MAP kinase activation is required for cell cycle progression. *Oncogene.* 17:1271–1277.
- Leppa, S., and D. Bohmann. 1999. Diverse functions of JNK signaling and c-Jun in stress response and apoptosis. *Oncogene.* 18:6158–6162.
- Liu, S., D.A. Calderwood, and M.H. Ginsberg. 2000. Integrin cytoplasmic domain-binding proteins. *J. Cell Sci.* 113:3563–3571.
- Meredith, J., Jr., Y. Takada, M. Fornaro, L.R. Languino, and M.A. Schwartz. 1995. Inhibition of cell cycle progression by the alternatively spliced integrin beta 1C. *Science.* 269:1570–1572.
- Mettouchi, A., S. Klein, W. Guo, M. Lopez-Lago, E. Lemichez, J.K. Westwick,

- and F.G. Giancotti. 2001. Integrin-specific activation of Rac controls progression through the G(1) phase of the cell cycle. *Mol. Cell.* 8:115–127.
- Oktyay, M., K.K. Wary, M. Dans, R.B. Birge, and F.G. Giancotti. 1999. Integrin-mediated activation of focal adhesion kinase is required for signaling to Jun NH2-terminal kinase and progression through the G1 phase of the cell cycle. *J. Cell Biol.* 145:1461–1469.
- Otey, C.A., G.B. Vasquez, K. Burridge, and B.W. Erickson. 1993. Mapping of the alpha-actinin binding site within the beta 1 integrin cytoplasmic domain. *J. Biol. Chem.* 268:21193–21197.
- Pfaff, M., S. Liu, D.J. Erle, and M.H. Ginsberg. 1998. Integrin beta cytoplasmic domains differentially bind to cytoskeletal proteins. *J. Biol. Chem.* 273:6104–6109.
- Retta, S.F., F. Balzac, P. Ferraris, A.M. Belkin, R. Fassler, M.J. Humphries, G. De Leo, L. Silengo, and G. Tarone. 1998. Beta1-integrin cytoplasmic subdomains involved in dominant negative function. *Mol. Biol. Cell.* 9:715–731.
- Roovers, K., G. Davey, X. Zhu, M.E. Bottazzi, and R.K. Assoian. 1999. Alpha5beta1 integrin controls cyclin D1 expression by sustaining mitogen-activated protein kinase activity in growth factor-treated cells. *Mol. Biol. Cell.* 10:3197–3204.
- Sastry, S.K., and A.F. Horwitz. 1993. Integrin cytoplasmic domains: mediators of cytoskeletal linkages and extra- and intracellular initiated transmembrane signaling. *Curr. Opin. Cell Biol.* 5:819–831.
- Sastry, S.K., M. Lakonishok, S. Wu, T.Q. Truong, A. Huttenlocher, C.E. Turner, and A.F. Horwitz. 1999. Quantitative changes in integrin and focal adhesion signaling regulate myoblast cell cycle withdrawal. *J. Cell Biol.* 144:1295–1309.
- Schaller, M.D., C.A. Otey, J.D. Hildebrand, and J.T. Parsons. 1995. Focal adhesion kinase and paxillin bind to peptides mimicking beta integrin cytoplasmic domains. *J. Cell Biol.* 130:1181–1187.
- Schlaepfer, D.D., S.K. Hanks, T. Hunter, and P. van der Geer. 1994. Integrin-mediated signal transduction linked to Ras pathway by GRB2 binding to focal adhesion kinase. *Nature.* 372:786–791.
- Wary, K.K., F. Mainiero, S.J. Isakoff, E.E. Marcantonio, and F.G. Giancotti. 1996. The adaptor protein Shc couples a class of integrins to the control of cell cycle progression. *Cell.* 87:733–743.
- Yang, J.T., H. Rayburn, and R.O. Hynes. 1993. Embryonic mesodermal defects in alpha 5 integrin-deficient mice. *Development.* 119:1093–1105.
- Yang, J.T., H. Rayburn, and R.O. Hynes. 1995. Cell adhesion events mediated by alpha 4 integrins are essential in placental and cardiac development. *Development.* 121:549–560.